Supporting Information

Li Vacancy-Induced Enhanced Ionic Conductivity in $Li_4B_7O_{12}Cl$ for All-solid-state Li-ion Battery

Shaowei Wang[1], Zesen Gao[1], Futing Sun[1], Yan Yang,[1] Lang Tao,[1] Yunluo Wang[1], Zhiqian Yu[2], Jianghua Wu[4], Jingshan Hou[4], Zhanqiang Liu[3], Hucheng Song[2], and Haijie Chen[1,*]

[1]*State Key Laboratory for Modification of Chemical Fibers and Polymer Materials, Institute of Functional Materials, College of Materials Science and Engineering, Donghua University, Shanghai, 201620, People's Republic of China*

[2]*National Laboratory of Solid-State Microstructures, School of Electronics Science and Engineering, Collaborative Innovation Center of Advanced Microstructures, Nanjing University, Nanjing, 210093, People's Republic of China*

[3]*Department of Materials Chemistry, Huzhou University, Huzhou 313000, People's Republic of China*

[4]*School of Materials Science and Engineering, Shanghai Institute of Technology, Shanghai, 201418, China*

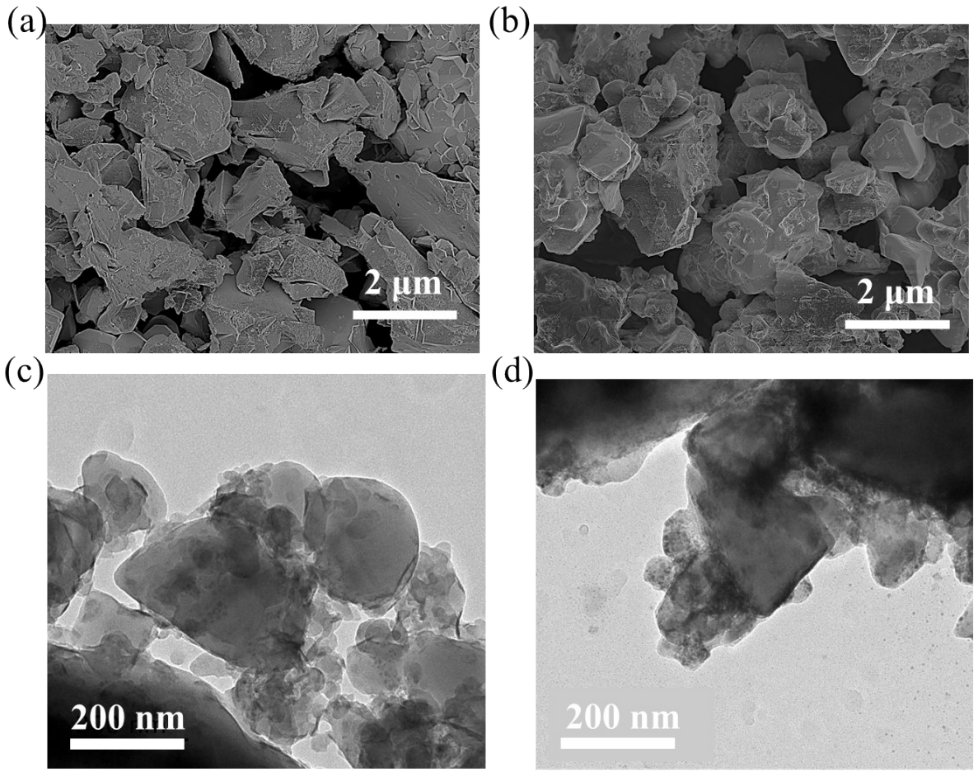

Figure S1. (a) The SEM image of $Li_4B_7O_{12}Cl$ solid state electrolyte. (b) The SEM image of $Li_{3.6}Mg_{0.2}B_7O_{12}Cl$ solid state electrolyte. (c) The TEM image of $Li_4B_7O_{12}Cl$ solid state electrolyte. (d) The TEM image of $Li_{3.6}Mg_{0.2}B_7O_{12}Cl$ solid state electrolyte.

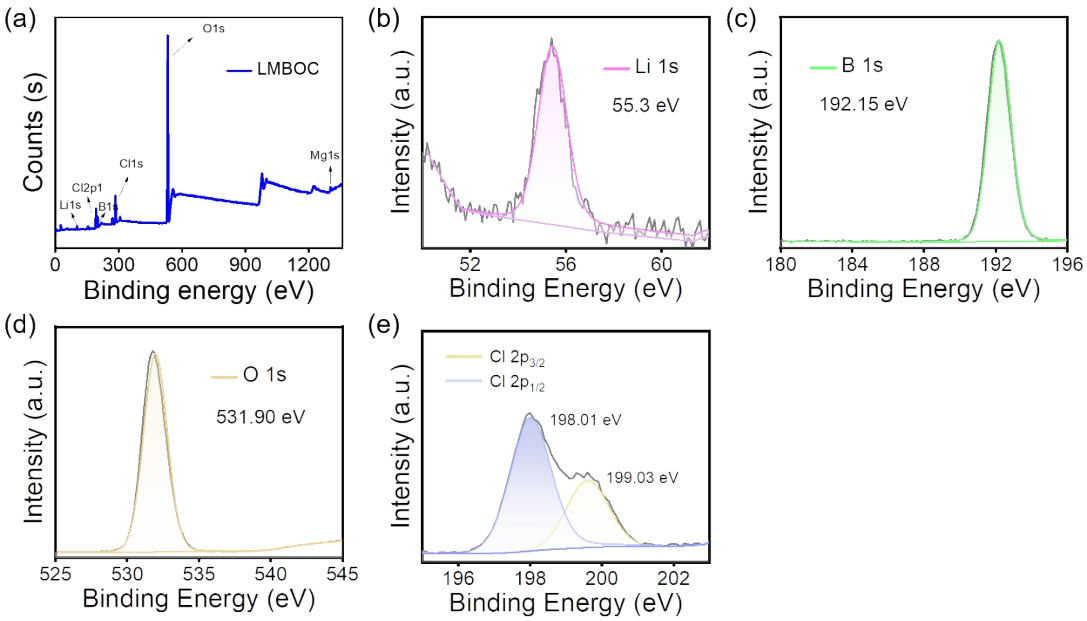

Figure S2. (a) XPS full spectrum of $Li_{3.6}Mg_{0.2}B_7O_{12}Cl$ (LMBOC). (b) Li 1s XPS spectra of $Li_{3.6}Mg_{0.2}B_7O_{12}Cl$. (c) B 1s XPS spectra of $Li_{3.6}Mg_{0.2}B_7O_{12}Cl$. (d) O 1s XPS spectra of $Li_{3.6}Mg_{0.2}B_7O_{12}Cl$. (e) Cl 2p XPS spectra of $Li_{3.6}Mg_{0.2}B_7O_{12}Cl$.

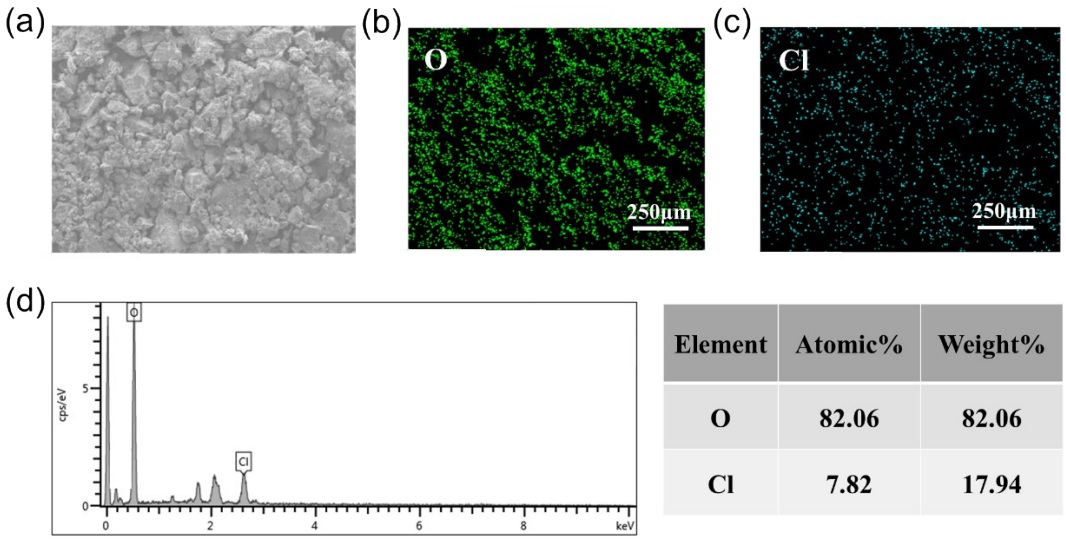

Element	Atomic%	Weight%
O	82.06	82.06
Cl	7.82	17.94

Figure S3. (a) The SEM image of $Li_4B_7O_{12}Cl$. (b-c) The corresponding elements EDS mappings of $Li_4B_7O_{12}Cl$ electrolyte (O and Cl). (d) The corresponding EDS spectrum at the indicated area and the results of EDS analysis of $Li_4B_7O_{12}Cl$.

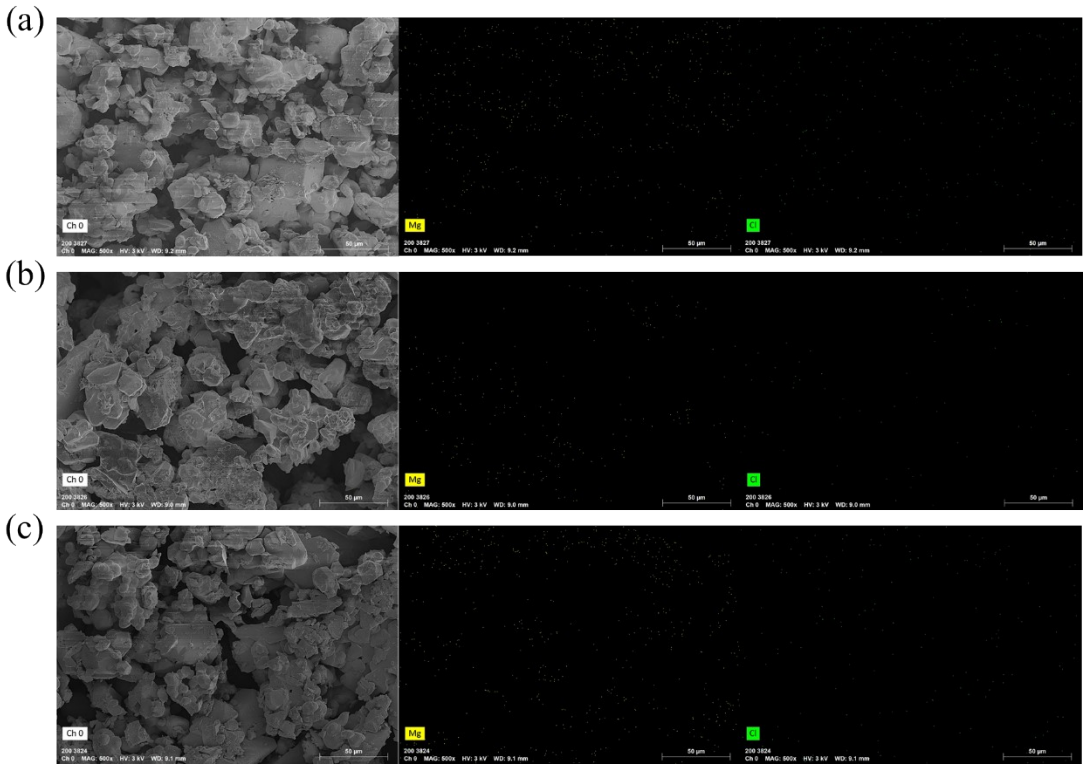

Figure S4. (a) The SEM image of $Li_{3.9}Mg_{0.05}B_7O_{12}Cl$ and the corresponding elements EDS mappings of $Li_{3.9}Mg_{0.05}B_7O_{12}Cl$ electrolyte (Mg, O, and Cl). (b) The SEM image of $Li_{3.8}Mg_{0.1}B_7O_{12}Cl$ and the corresponding elements EDS mappings of $Li_{3.8}Mg_{0.1}B_7O_{12}Cl$ electrolyte (Mg, O, and Cl). (c) The SEM image of $Li_{3.7}Mg_{0.15}B_7O_{12}Cl$ and the corresponding elements EDS mappings of $Li_{3.7}Mg_{0.15}B_7O_{12}Cl$ electrolyte (Mg, O, and Cl).

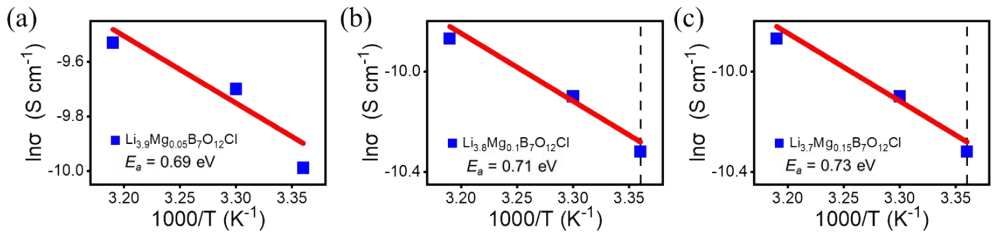

Figure S5. (a) Arrhenius diagram of $Li_{3.9}Mg_{0.05}B_7O_{12}Cl$ based on temperature and electrochemical impedance spectroscopy. (b) Arrhenius diagram of $Li_{3.8}Mg_{0.1}B_7O_{12}Cl$ based on temperature and electrochemical impedance spectroscopy. (c) Arrhenius diagram of $Li_{3.7}Mg_{0.15}B_7O_{12}Cl$ based on temperature and electrochemical impedance spectroscopy.

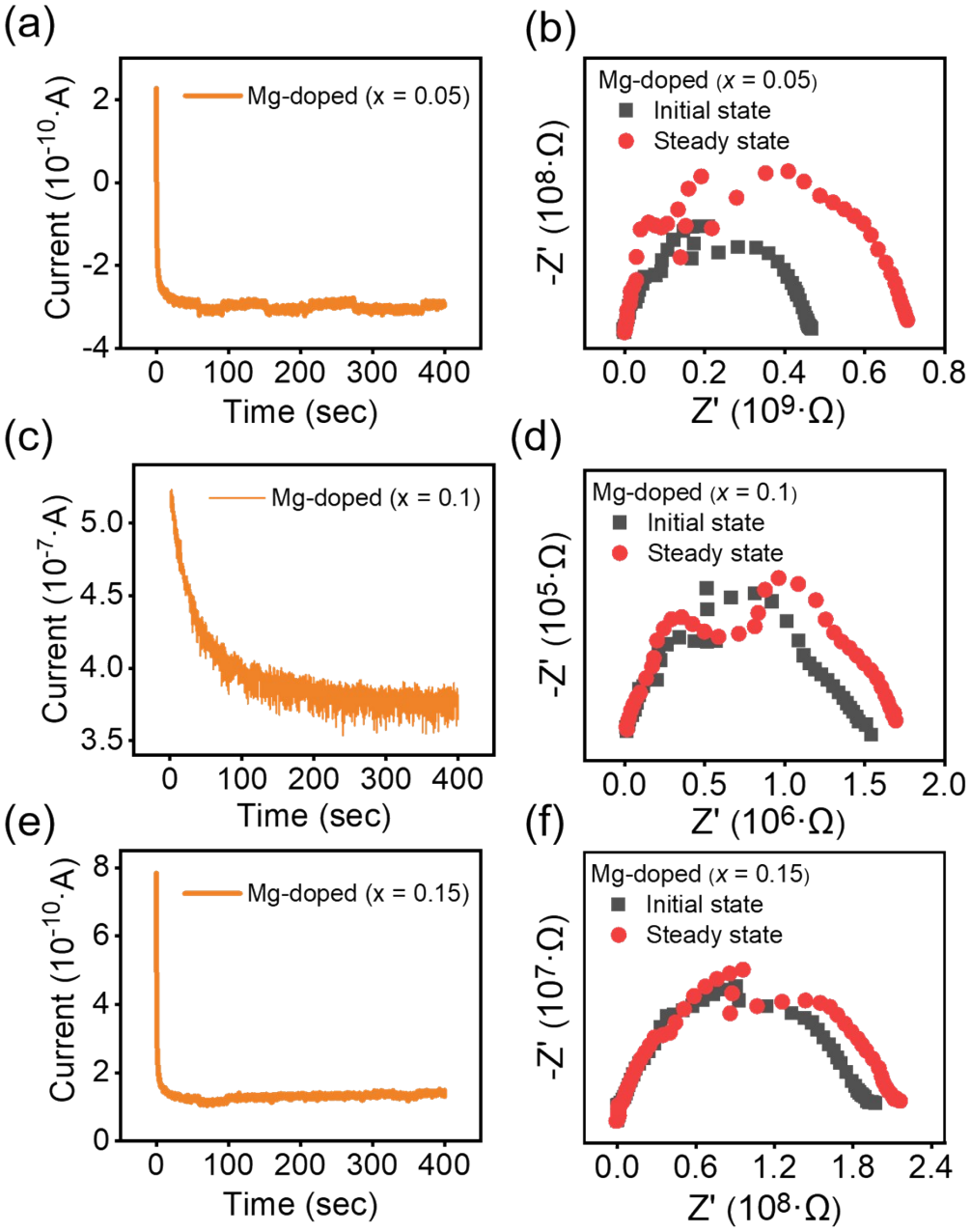

Figure S6. Chronoamperometry measurements for the $Li_{4-2x}Mg_xB_7O_{12}Cl$ electrolytes-based lithium symmetric batteries ((a) $x = 0.05$, (c) $x = 0.1$, and (e) $x = 0.15$)). Nyquist impedance plots of the $Li_{4-2x}Mg_xB_7O_{12}Cl$ electrolytes before and after polarization ((b) $x = 0.05$, (d) $x = 0.1$, and (f) $x = 0.15$)).

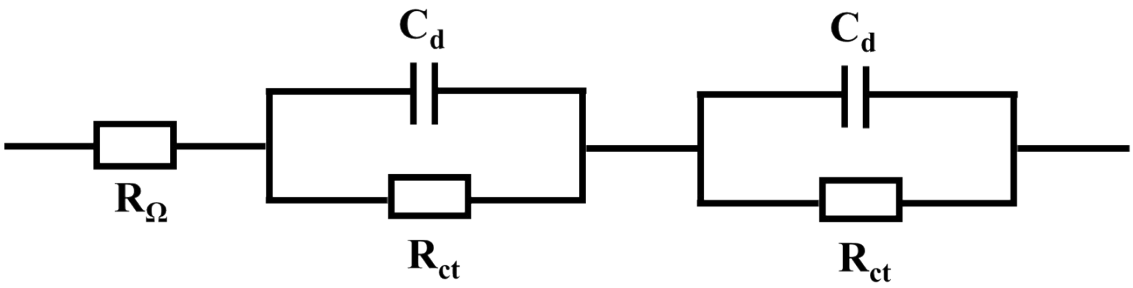

Figure S7. The equivalent circuit for fitting the EIS spectra of the Li | $Li_{4-2x}Mg_xB_7O_{12}Cl$ | Li cell.

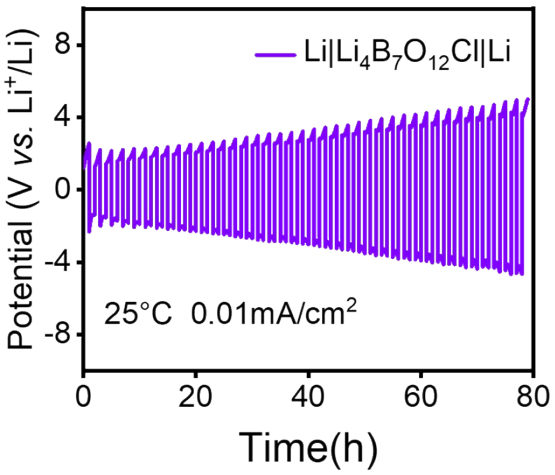

Figure S8. The galvanostatic charge−discharge cycle measurement of the ($Li|Li_4B_7O_{12}Cl|Li$) cell at a current density of 0.01 mA/cm^2 at room temperature.

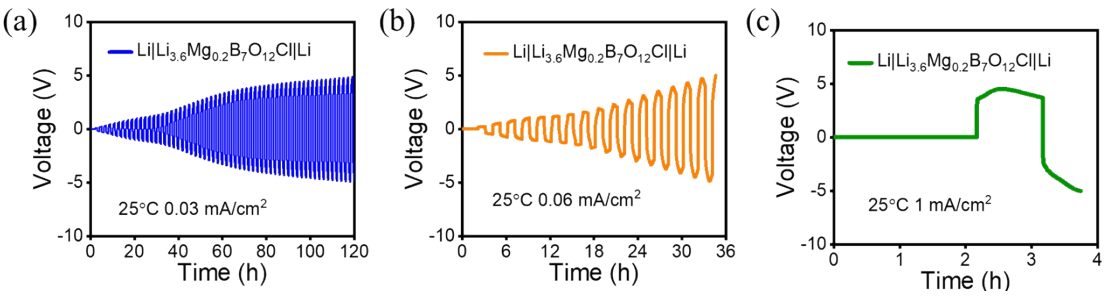

Figure S9. (a) The galvanostatic charge−discharge cycle measurement of the (Li| $Li_{3.6}Mg_{0.2}B_7O_{12}Cl$ |Li) cell at a current density of 0.03 mA/cm^2 at room temperature. (b) The galvanostatic charge−discharge cycle measurement of the (Li| $Li_{3.6}Mg_{0.2}B_7O_{12}Cl$ |Li) cell at a current density of 0.06 mA/cm^2 at room temperature. (c) The galvanostatic charge−discharge cycle measurement of the (Li| $Li_{3.6}Mg_{0.2}B_7O_{12}Cl$ |Li) cell at a current density of 1 mA/cm^2 at room temperature.

Table S1. Structural data for $Li_4B_7O_{12}Cl$.

Atom	Wyckoff	Atomic coordinates			*Occ.*	U
		x	y	z		
Cl	8b	0.25	0.25	0.25	1	1
B	24d	0.25	0	0	1	1
B	32e	0.10036	0.10036	0.10036	1	1
O	96h	0.02252	0.09813	0.18172	1	1
Li	32e	0.8708	0.8708	0.8708	0.25	1
Li	24c	0	0.25	0.25	1	1

Table S2. Structural data for $Li_{3.6}Mg_{0.2}B_7O_{12}Cl$ obtained from Rietveld refinement.

Atom	Wyckoff	Atomic coordinates			*Occ.*	U
		x	y	z		
Cl	8b	0.25	0.25	0.25	1	0.418
B	24d	0.25	0	0	1	0.406
B	32e	0.0986	0.0986	0.0986	1	0.391
O	96h	0.0231	0.096	0.1807	1	0.398
Li	32e	0.844	0.844	0.844	0.25	0.75
Li	24c	0	0.25	0.25	0.8	0.548
Mg	24c	0	0.25	0.25	0.2	0.548
Mg	32e	0.844	0.844	0.844	0.25	0.75

Table S3. The result of ICP-OES measurement.

Sample	Mg content (%, ICP)	Mg precursors content (%)
$\mathbf{Li_{3.6}Mg_{0.2}B_7O_{12}Cl}$	0.198	0.2

$$Mg\ Content = \frac{Mg\ Concentration\ measured\ by\ ICP}{Li\ Concentration\ measured\ by\ ICP} \times 100\%$$

Table S4. The results of EDS mappings of $Li_{4-2x}Mg_xB_7O_{12}Cl$ (x = 0.05, 0.10, 0.15) electrolyte (Mg, and Cl).

Material	Atom ratio	
	Mg	**Cl**
$Li_{3.9}Mg_{0.05}B_7O_{12}Cl$	4.82	95.18
$Li_{3.8}Mg_{0.1}B_7O_{12}Cl$	9.4	90.6
$Li_{3.7}Mg_{0.15}B_7O_{12}Cl$	13.2	86.8